Journal of Alloys and Compounds 489 (2010) 384–388

Contents lists available at ScienceDirect

Journal of Alloys and Compounds

journal homepage: www.elsevier.com/locate/jallcom

The phase relationships in the Gd–Ti–Sn ternary system at 473 K and the new compound $GdSn_4Ti_6$

Jianbo Ma[a], Yongzhong Zhan[a,*], Jia She[a], Zhulin Yang[a], Jianlie Liang[b]

[a] Laboratory of Nonferrous Metal Materials and New Processing Technology, Ministry of Education, Guangxi University, Nanning, Guangxi 530004, PR China
[b] Institute of Materials Science, College of Physics and Electronic Engineering, Guangxi University for Nationalities, Nanning, Guangxi 530006, PR China

ARTICLE INFO

Article history:
Received 14 July 2009
Received in revised form
16 September 2009
Accepted 16 September 2009
Available online 25 September 2009

Keywords:
Phase diagrams
Metal alloys
X-ray diffraction

ABSTRACT

The phase relationships in the Gd–Ti–Sn ternary system at 473 K have been investigated mainly by means of X-ray powder diffraction (XRD). Twelve binary compounds, i.e. Gd_5Sn_3, Gd_5Sn_4, $Gd_{11}Sn_{10}$, $GdSn_2$, Gd_3Sn_7, Gd_4Sn_{11}, $GdSn_3$, Ti_3Sn, Ti_2Sn, Ti_5Sn_3, Ti_6Sn_5 and Ti_2Sn_3 were confirmed. A new ternary compound $GdSn_4Ti_6$ was found with space group $R\bar{3}m$ and lattice parameters $a = 0.57857$ nm, and $c = 2.27976$ nm (Gd occupying the 3*a* positions, Sn occupying the two 6*c* positions and Ti occupying the 18*h* positions). The isothermal section of the Gd–Ti–Sn ternary system at 473 K consists of 16 single-phase regions, 30 two-phase regions and 15 three-phase regions.

1. Introduction

It is well known that titanium and titanium alloys have high strength and hardness, outstanding mechanical properties, corrosion resistance, etc.; as a result they have got more and more attentions [1,2]. Complex alloying method is considered to be one of the important ways to improve and make use of the excellent properties of Ti alloys and step up their practical applications. The previous works have shown that Sn can significantly increase the strength and corrosion resistance of Ti alloys [3,4]. Addition of small amount of a rare earth element to improve the microstructures and properties of titanium alloys has been studied [5,6]. In order to discover further characteristics and regularities concerning phase formation in the Gd–Ti–Sn ternary system, it is necessary to investigate the phase relationships in this system.

Gd–Ti and Ti–Sn systems have been studied in the previous works [7–9]. There is no binary compound in the Gd–Ti system and five intermediate compounds, i.e. Ti_3Sn, Ti_2Sn, Ti_5Sn_3, Ti_6Sn_5 and Ti_2Sn_3 are reported in the Ti–Sn system. It is reported that there are seven binary compounds, namely Gd_5Sn_3, Gd_5Sn_4, $Gd_{11}Sn_{10}$, $GdSn_2$, Gd_3Sn_7, Gd_4Sn_{11} and $GdSn_3$ in Ref. [10]. However, the Gd–Sn binary phase diagram [11] indicates that there are three other compounds, i.e. Gd_3Sn, Gd_8Sn_7 and Gd_3Sn_4 exist. The investigation of Gd–Fe–Sn ternary phase diagram [12] did not show the existence of the three compounds at 670 K and 870 K. Ref. [13] shows that the compound Gd_4Sn_{11} does not exist. In Refs. [14,15], the compound Gd_4Sn_{11} was not listed in the Gd–Sn and Gd–Fe–Sn phase diagrams. In this work, the phase relation of Gd–Ti–Sn system at 473 K has been investigated.

2. Experimental

All the 125 alloy buttons were produced by arc melting on a water-cooled copper cast with a non-consumable tungsten electrode under pure argon atmosphere. Titanium was used as an O_2 getter during the melting process. Each sample was prepared with a total weight of 1.5 g by weighting appropriate of the pure components (Gd: 99.95 wt.%; Ti: 99.99 wt.%; Sn: 99.95 wt.%). Each arc-cast button had been melted three times and turned around after melting for better homogeneity. The homogenization temperature was determined by differential thermal analysis (DTA). For most alloys, the weight loss is less than 1% after melting.

All the melted alloy buttons were sealed in evacuated quartz tubes for homogenization heat treatment. The alloys at the Sn rich corner were homogenized at 473 K for 960 h and the rest alloys were homogenized at 1043 K for 360 h, then they were cooled down to 473 K at a rate of 9 K/h and maintained for more than 240 h. Finally, all these annealed buttons were quenched in liquid nitrogen.

Finally, the equilibrated samples were ground into powder and then analyzed on a Rigaku D/Max-2500 V diffractometer with Cu Kα radiation and graphite monochromator. The scanning range of the new compound $GdSn_4Ti_6$ was from 10° to 110° (2θ) with a step size of 0.02° and a count time of 2 s per step. The rest of the samples were from 20° to 60° (2θ) with a speed of 10° per minute. The software Jade 5.0 and Powder Diffraction File (PDF release 2003) were used for phase identification [16]. Scanning electron microscopy (SEM) (HITACHI S-3400N) with energy dispersive spectrometer (EDS) was used for microstructural analysis in this work. The magnetization measurement for $GdSn_4Ti_6$ was carried out using a vibrating sample magnetometer (VSM, Lakeshore 7410).

* Corresponding author at: Institute of Materials Science, School of Materials Science and Enigineering, Daxue Road, 100, Nanning, Guangxi 530004, PR China.
E-mail address: zyzmatres@yahoo.com.cn (Y. Zhan).

0925-8388/$ – see front matter © 2009 Elsevier B.V. All rights reserved.
doi:10.1016/j.jallcom.2009.09.106

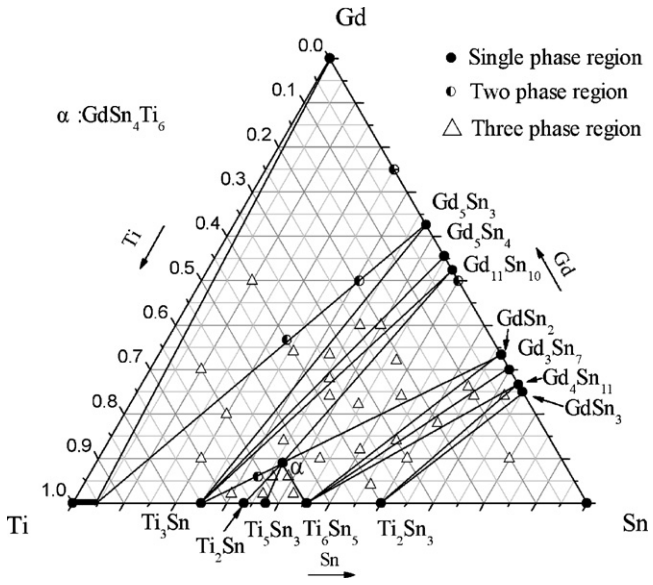

Fig. 1. The 473 K isothermal section of the Gd–Ti–Sn ternary system.

3. Results and discussion

3.1. Isothermal section

Based on the result of phase analysis of XRD patterns of all the samples, the 473 K isothermal section of the Gd–Ti–Sn ternary system was determined, as shown in Fig. 1. The isothermal section consists of 16 single-phase regions, 30 two-phase regions and 15 three-phase regions. The compositions of the typical alloys of the Gd–Ti–Sn system at 473 K are shown in Fig. 1, too.

3.2. Phase analysis

In the Gd–Ti system, it has been confirmed that there is no intermediate compound at 473 K in this work. In the Ti–Sn system, all the five binary compounds, i.e. Ti_3Sn, Ti_2Sn, Ti_5Sn_3, Ti_6Sn_5 and Ti_2Sn_3 have been confirmed at 473 K, which agrees well with the previous work [8,9]. The seven binary compounds, namely Gd_5Sn_3, Gd_5Sn_4, $Gd_{11}Sn_{10}$, $GdSn_2$, Gd_3Sn_7, Gd_4Sn_{11} and $GdSn_3$ in the Gd–Sn system were confirmed at 473 K in this work. The compounds Gd_3Sn, Gd_8Sn_7 and Gd_3Sn_4 were not found, which agrees well with Ref. [12]. The XRD pattern of the alloy with the atomic proportion Gd 50% and Sn 50% (shown in Fig. 2) shows that there is no Gd_8Sn_7 and Gd_3Sn_4 phase. A new ternary compound $GdSn_4Ti_6$ was found. All the crystal structure data of intermediate compounds in the Gd–Ti–Sn system at 473 K are shown in Table 1.

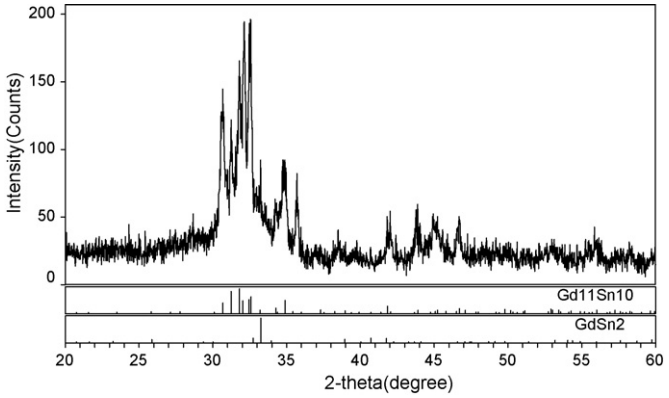

Fig. 2. The XRD pattern of the alloy with the atomic proportion of Gd 50% and Sn 50%.

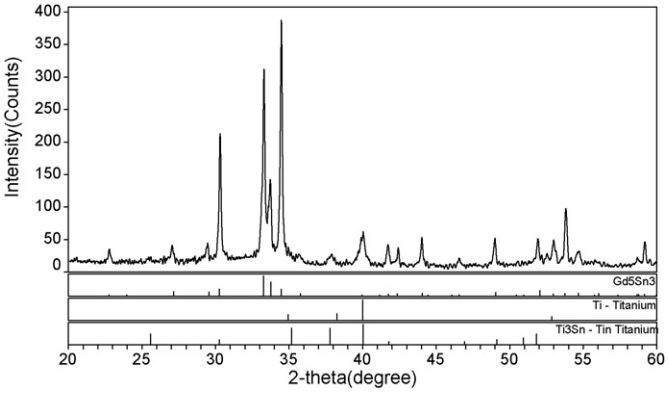

Fig. 3. The XRD pattern of the equilibrated sample prepared with atomic proportion Gd 34%, Sn 26% and Ti 40%.

Based on the analysis of the details of the XRD patterns (shown in Fig. 3.) of the equilibrated sample prepared with the atomic proportion Gd 34%, Sn 26% and Ti 40%, the binary compound Gd_5Sn_3 can be confirmed, and the three-phase region $Gd_5Sn_3 + Ti + Ti_3Sn$ can be determined. The detail of the XRD pattern of the equilibrated sample with the atomic proportion Gd 33.3%, Sn 33.4% and Ti 33.3% (shown in Fig. 4.) shows that there are three phases, i.e. Gd_5Sn_3, Gd_5Sn_4 and Ti_3Sn, so the corresponding three-phase region can be determined. The intermediate compounds Gd_4Sn_{11}, Ti_2Sn_3 and Ti_6Sn_5 were confirmed based on the XRD analysis of the equilibrated alloy with the atom proportion Gd 4%, Sn 56% and Ti 40%

Table 1
The crystal structure data of intermediate compounds in the Gd–Ti–Sn system at 473 K.

Compound	Space group	Lattice parameters (nm)			Reference
		a	*b*	*c*	
Gd_5Sn_3	$P6_3/mcm$	0.9020	–	0.6568	[10]
Gd_5Sn_4	*Pnma*	0.8040	1.553	0.8192	[10]
$Gd_{11}Sn_{10}$	$I4/mmm$	1.167		1.715	[10]
$GdSn_2$	*Cmcm*	0.4428	1.6410	0.4322	[10]
Gd_3Sn_7	*Cmmm*	0.44597	2.65163	0.43823	[10]
Gd_4Sn_{11}	*Amm*2	0.43552	0.44039	2.2044	[10]
$GdSn_3$	$Pm\bar{3}m$	0.46775	–	–	[10]
Ti_3Sn	$P6_3/mmc$	0.5916	–	0.4764	[10]
Ti_2Sn	$P6_3/mmc$	0.4653	–	0.5700	[10]
Ti_5sn_3	$P6_3/mcm$	0.8049	–	0.5454	[10]
Ti_6Sn_5	$P6_3/mmc$	0.922	–	0.569	[10]
Ti_2Sn_3	*Cmca*	0.596	1.994	0.702	[8,9]
$GdSn_4Ti_6$	$R\bar{3}m$	5.7857	–	22.7976	This work

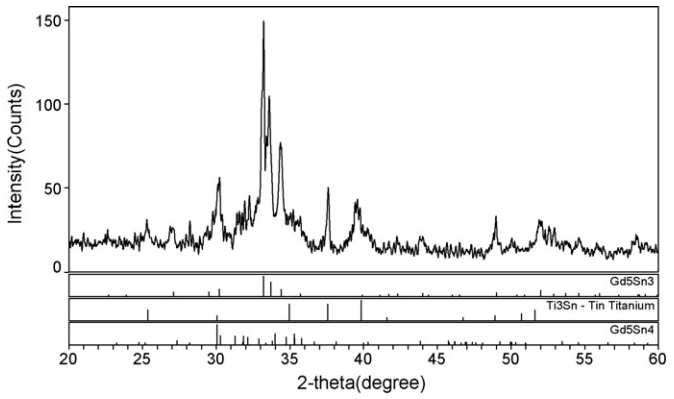

Fig. 4. Detail of the XRD pattern of the equilibrated sample with atomic proportion Gd 4%, Sn 56% and Ti 40%.

(shown in Fig. 5). The rest binary compounds can be confirmed by the same method.

The solid solubility ranges of the single phases were determined using the phase-disappearing method and comparing the shift of the XRD patterns of the samples near to the compositions of the binary phases [17]. The results indicate that all the intermediate compounds in this system do not have a remarkable solid solution at 473 K. The solubility of Sn in the α-Ti phase at 473 K is determined to be 5%, which is in well agreement with that in the Ti–Sn phase diagram [18].

3.3. The new compound $GdSn_4Ti_6$

3.3.1. Crystal structure of $GdSn_4Ti_6$

In analyzing the XRD patterns of the alloys with stoichiometric composition around Gd 10%, Sn 36.8% and Ti 53.2%, there are always some strong diffraction peaks at degrees about 31, 35, 39 and so on. This cannot be explained by the reported phases Ti_6Sn_5, Ti_5Sn_3, Ti_2Sn, Ti_3Sn, $GdSn_2$ and $Gd_{11}Sn_{10}$. The alloy with the atomic proportion of Gd 6%, Sn 33% and Ti 61% was prepared in this work. The detail of the XRD pattern and the SEM micrograph (shown in Fig. 6.) of the alloy show that it just has two phases, i.e. Ti_3Sn and a new phase ($GdSn_4Ti_6$). Energy dispersive spectrometer (EDS) analysis was employed to identify the new phase. Because of the extending effect of the electronic bundles, the results of EDS (shown in Fig. 7) show that the phase contained Gd 12.22 at.%, Sn 36.62 at.% and Ti 51.15 at.%. Some samples near to this composition were prepared, and the single phase was obtained at the compositional point of Gd 10 at.%, Sn 36.8 at.% and Ti 53.2 at.%. The XRD pattern of the single phase could be indexed using Jade 5.0. The results indicate that the

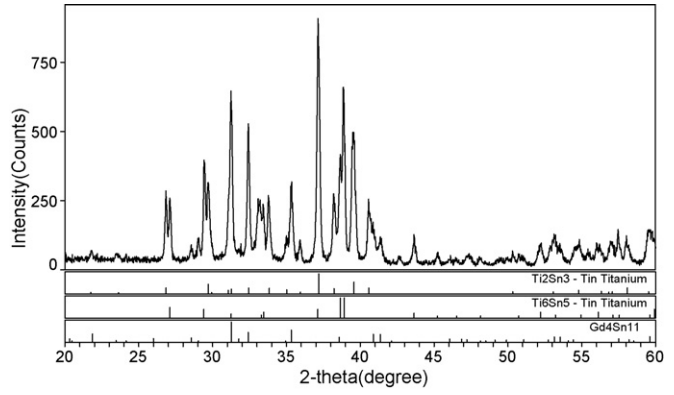

Fig. 5. The XRD pattern of the equilibrated sample with the atomic proportion of Gd 33.3%, Sn 33.4% and Ti 33.3%.

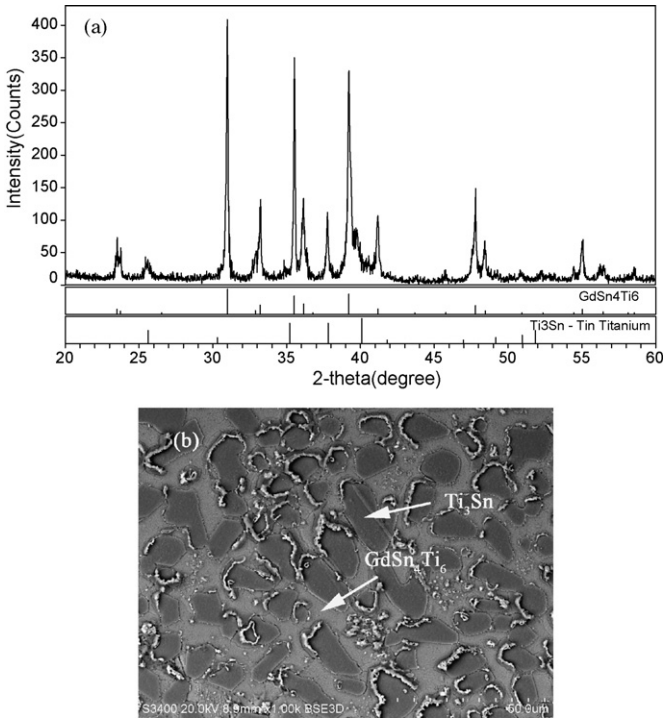

Fig. 6. The XRD pattern (a) and the SEM micrograph (b) of the equilibrated alloy containing Gd 6%, Sn 33% and Ti 61%.

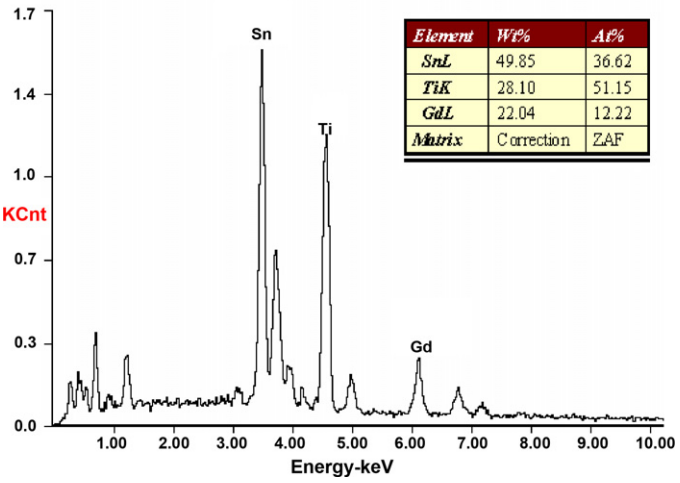

Fig. 7. EDS pattern of the new phase shows that the phase contains Gd 12.22 at.%, Sn 36.62 at.% and Ti 51.15 at.%.

new phase has a trigonal structure with space group $R\bar{3}m$ (no. 166) or R3m (no. 160) or R32 (no. 155) and parameters of $a = 0.5791$ nm, $c = 2.2824$ nm, and Vol = 0.66285 nm^3.

Each space group was attempted in this work, and the Rietveld's method was used to analyze the X-ray powder diffraction patterns of the new phase. In the end, the structure (Gd occupying the 3*a* positions, Sn occupying the two 6*c* positions and Ti occupying the

Table 2
Atomic parameters of $GdSn_4Ti_6$.

Element	Positions	*x*	*y*	*z*	Occ.
Gd	3*a*	0	0	0	1
Sn	6*c*	0	0	0.33229	1
Sn	6*c*	0	0	0.12791	1
Ti	18*h*	0.49516	0.50484	0.10684	1

Table 3
Rietveld structural refinement data of $GdSn_4Ti_6$.

Space group	$R\bar{3}m$ (no. 166)
Cell parameters	$a = b = 0.57857$ nm, $c = 2.27976$ nm, $\alpha = \beta = 90^\circ$, $\gamma = 120^\circ$
Volume of unit cells (nm^3)	0.660893
Calculated density (g/cm^3)	7.021
Reliability factors (*R*-factor)	$R_P = 10.51\%$, $R_{WP} = 13.44\%$, $R_{EXP} = 5.78\%$

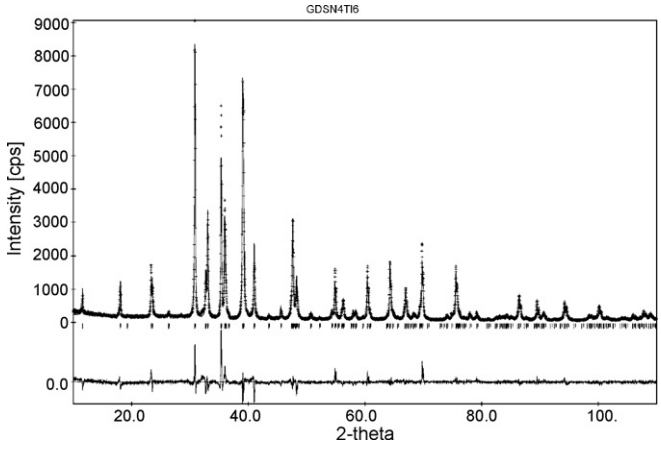

Fig. 8. The XRD pattern of $GdSn_4Ti_6$. (+, observed patterns; the solid line, calculated patterns; |, the possible positions of Bragg reflections; the bottom curves, the difference between the observed and calculated patterns).

18*h* positions, shown in Table 2) with the space group $R\bar{3}m$ (no. 166) can well explain the XRD pattern. The structural refinement was performed using the DBWS9807 program [19]. The Pseudo-Voigt function was used for the simulation of the peak shapes. The

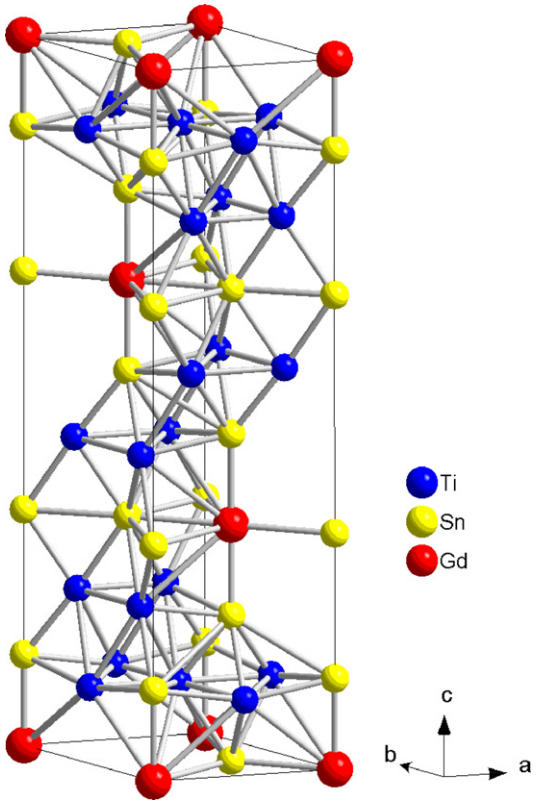

Fig. 9. The crystal structure of $GdSn_4Ti_6$.

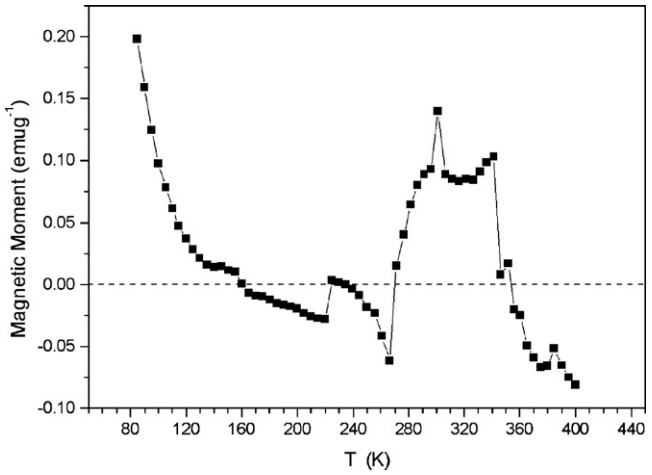

Fig. 10. The thermal dependence of the magnetization (*M*–*T*) curves for $GdSn_4Ti_6$.

DMPLOT-plot view program [20] was used to follow the refinement results. The key contents of the Rietveld structural refinement are presented in Table 3. The pattern *R*-factor (R_p) and the weighted pattern *R*-factor (R_{wp}) are $R_p = 0.1051$ and $R_{wp} = 0.1344$, respectively. The observed, calculated data and differences of the powder diffraction patterns of the new phase are shown in Fig. 8. In the end, the authors signed the new phase as $GdSn_4Ti_6$. The crystal structure of $GdSn_4Ti_6$ is given in Fig. 9.

3.3.2. *Magnetic property of $GdSn_4Ti_6$*

Fig. 10 shows the thermal dependence of the magnetization (*M*–*T*) curve for $GdSn_4Ti_6$ measured in a temperature range from 85 K to 400 K under an applied field of 0.1 T. Between 85 K and 160 K, the compound is paramagnetism. The compound shows diamagnetism between 160 K and 270 K and antiferromagnetic between 270 K and 345 K with the Néel temperature of 300 K. Between 350 K and 400 K, the compound shows diamagnetism.

4. Conclusions

In this work, 12 binary compounds, i.e. Gd_5Sn_3, Gd_5Sn_4, $Gd_{11}Sn_{10}$, $GdSn_2$, Gd_3Sn_7, Gd_4Sn_{11}, $GdSn_3$, Ti_3Sn, Ti_2Sn, Ti_5Sn_3, Ti_6Sn_5 and Ti_2Sn_3 were confirmed. A new ternary compound $GdSn_4Ti_6$ was found with space group $R\bar{3}m$ (no. 166) and lattice parameters $a = 0.57857$ nm, and $c = 2.27976$ nm (Gd occupying the 3*a* positions, Sn occupying the two 6*c* positions and Ti occupying the 18*h* positions). The isothermal section of the Gd–Ti–Sn ternary system at 473 K consists of 16 single-phase regions, 30 two-phase regions and 15 three-phase regions.

Acknowledgements

The authors wish to express thanks to the financial support from the National Natural Science Foundation of China (50601006, 50761003), the Key Project of China Ministry of Education (207085).

References

[1] Y. Zhan, Z. Yu, Y. Wang, Y. Xu, X. Shi, Tribol. Lett. 26 (2007) 25–31.
[2] M. Bulanova, L. Tretyachenko, K. Meleshevich, V. Saltykov, V. Vereshchaka, O. Galadzhyj, L. Kulak, S. Firstov, J. Alloys Compd. 350 (2003) 164–173.
[3] J.W. Suiter, J. Inst. Met. 84 (1955) 81–86.
[4] I.I. Kornilov, T.T. Nartova, J. Inorg. Chem. 5 (1960) 622–624.
[5] Y. Liu, L. Chen, W. Wei, H. Tang, B. Liu, B. Huang, J. Mater. Sci. Technol. 22 (2006) 465–469.
[6] K. Xia, W. Li, C. Liu, Scripta Mater. 41 (1999) 67–73.
[7] Y. Zhan, J. Ma, Z. Sun, Z. Hu, Y. Du, J. Alloys Compd. 475 (2009) 268–272.

[8] Y. Zhan, Y. Xu, H. Xie, Z. Yu, Y. Wang, Y. Zhuang, J. Alloys Compd. 459 (2008) 174–176.
[9] Y. Zhan, L. He, J. Ma, Z. Sun, G. Zhang, Y. Zhuang, J. Alloys Compd. 470 (2009) 173–175.
[10] P. Villars, Pearson's Handbook of Crystallographic Data, ASM International, Materials Park, OH, 1997.
[11] A. Palenzona, S. Cirafici, J. Phase Equilib. 12 (1991) 691–695.
[12] Y. Mudryk, L. Romaka, Y. Stadnyk, O. Bodak, D. Fruchart, J. Alloys Compd. 383 (2004) 162–165.
[13] A. Palenzona, P. Manfrinetti, J Alloys Compd. 201 (1993) 43–47.
[14] H. Okamoto, J. Phase Equilib. 16 (1995) 100–101.
[15] V. Raghavan, J. Phase Equilib. Diff. 2 (2007) 387–388.
[16] Materials Data JADE Release 5.0, XRD Pattern Processing, Materials Data Inc., Livermore, CA, 2003.
[17] Y. Zhan, Y. Du, Y. Zhuang, in: J.-C. Zhao (Ed.), Methods for Phase Diagram Determination, first ed., Elsevier Science Press, Amsterdam, The Netherlands, 2007, pp. 108–150.
[18] J.L. Murray, Phase Diagrams of Binary Titanium Alloys, 1987.
[19] R.A. Young, A.C. Larson, C.O. Paiva-Santos, User's Guide to Program DBWS-9807a for Rietveld Analysis of X-ray and Neutron Powder Diffraction Patterns with a PC and various other computers, School of Physics, Georgia Institute of Technology, Atlanta, GA, 1998.
[20] H. Marciniak, R. Diduszko, DMPLOT-Plot view program for Rietveld refinement method, Version 3 Computer Software, 1997.